scientific reports

Check for updates

OPEN

A novel hybridization of birds of prey-based optimization with differential evolution mutation and crossover for chaotic dynamics identification

Serdar Ekinci[1], Davut Izci[2,3]✉, Murat Kayri[4], Fahmi Elsayed[5] & Mohammad Salman[5]

Parameter identification of chaotic systems such as Lorenz, Chen, and Rössler has long been recognized as a challenging inverse problem, since even slight perturbations in system coefficients can yield qualitatively different trajectories. Conventional time-domain error formulations are often ill-conditioned under these conditions, which has motivated the design of more robust objective functions and the adoption of metaheuristic optimization strategies. In this study, a hybrid birds of prey-based optimization with differential evolution (h-BPBODE) is introduced to address these challenges. The method enriches the four canonical behavioral phases of BPBO (individual hunting, group hunting, attacking the weakest, and relocation) by embedding DE mutation and crossover operators after each candidate update. This design injects recombinative diversity while retaining BPBO's adaptive and collective search mechanisms, thereby improving the balance between exploration and exploitation. The algorithm is validated on Lorenz, Chen, and Rössler systems, where the task is to recover unknown parameters by minimizing trajectory mismatches between true and simulated models. Comparative simulations against standard BPBO, starfish optimization, hippopotamus optimization, particle swarm optimization (PSO), and DE confirm that h-BPBODE consistently achieves exact parameter recovery with negligible residuals, faster convergence, and markedly lower run-to-run variance. Statistical analyses, convergence traces, and parameter evolution curves further demonstrate its robustness and precision. These findings establish h-BPBODE as a reliable and efficient framework for chaotic system identification and suggest its potential for broader nonlinear estimation tasks.

Keywords Birds of prey-based optimization, Chaotic systems, Parameter identification, Mutation and crossover operators, Differential evolution, Hybridization

Identifying the parameters of canonical chaotic flows (Lorenz, Chen, and Rössler) has long been regarded as a demanding inverse problem in nonlinear dynamics[1]. Small perturbations in the coefficients can induce large deviations in state trajectories, so conventional time-domain error criteria often become ill-conditioned and prone to local minima. Prior work has addressed this difficulty from two directions: by designing better-posed objective functions (e.g., return-map/Poincaré-based costs that preserve geometric invariants), and by deploying metaheuristic search to escape poor basins of attraction[1–3]. Together, these threads shifted the focus from purely deterministic estimators toward stochastic, diversity-preserving optimization schemes tailored to chaotic identification.

Parameter identification in canonical chaotic flows such as Lorenz, Chen, and Rössler remains a fundamental challenge in nonlinear dynamics. Traditional time-domain error minimization functions are often ill-conditioned, since sensitive dependence on initial conditions destroys trajectory similarity. Jafari et al. addressed

[1]Department of Computer Engineering, Bitlis Eren University, 13100 Bitlis, Turkey. [2]Department of Electrical and Electronic Engineering, Bursa Uludag University, 16059 Bursa, Turkey. [3]Applied Science Research Center, Applied Science Private University, Amman 11931, Jordan. [4]Department of Computer and Instructional Technology Education, Van Yuzuncu Yil University, Van, Turkey. [5]College of Engineering and Technology, American University of the Middle East, Egaila 54200, Kuwait. ✉email: davutizci@gmail.com; davutizci@uludag.edu.tr

this by proposing a return-map/Poincaré-based cost function, demonstrating on Lorenz and other flows that geometric invariants yield a monotone objective surface robust to noise[2]. This insight paved the way for coupling better-posed cost functions with metaheuristic search strategies.

Among early metaheuristics, genetic algorithms (GA) and particle swarm optimization (PSO) were widely applied, yet suffered from local entrapment and premature convergence. Hybrid improvements proved more effective: Ko et al. introduced hybrid evolutionary quantum-behaved particle swarm optimization (HEQPSO), a quantum-behaved PSO enriched with GA mutation and simulated annealing, achieving superior parameter estimation accuracy for Lorenz, Chen, and Rössler compared to GA, PSO, and hybrid differential evolution (DE) variants[4]. Chang et al. combined adaptive cuckoo search (ACS) with PSO, forming ACS–PSO, which significantly outperformed its components on Lorenz estimation, highlighting the exploration–exploitation balance of hybrid methods[5].

Recent algorithmic innovations have further diversified the field. Ebrahimi et al. proposed the improved Lozi-map chaotic optimization algorithm (ILCOA), demonstrating that chaotic search dynamics can enhance the balance of intensification and diversification; on Lorenz and Chen benchmarks, ILCOA outperformed DE, PSO, and artificial bee colony (ABC)[6]. Likewise, Turgut et al. embedded cellular automata structures into whale optimization algorithm (WOA) and sine–cosine algorithm (SCA), producing cellular WOA/SCA. Tested on Lorenz, Chen, Rössler, and Duffing systems, these cellular variants achieved faster convergence and higher robustness than their standard forms or classic PSO/DE competitors[7]. Chen, Pi and Wang enhanced the flower pollination algorithm (FPA) with chaotic mapping and DE-style local perturbations, producing the global flower pollination algorithm (GFPA), which achieved zero-error parameter identification on Lorenz, Chen, and Rössler, as well as hyper-chaotic extensions[8]. In parallel, Zainel et al. introduced a quantum fruit fly optimization algorithm (QFOA), applying quantum probability search to Lorenz, Chen, and Rössler systems; QFOA delivered superior convergence and reliability compared to GA, PSO, and cuckoo search (CS)[9].

Beyond single-system tests, broader frameworks have evaluated algorithms using chaos-theoretic criteria. Moreno-López et al. optimized Lorenz, Chen, and Rössler to maximize the Kaplan–Yorke dimension, validating chaos intensity while applying results to FPGA-based pseudo-random number generators[10]. Their statistical comparisons (Wilcoxon, Levene) confirmed the competitive advantage of DE, grey wolf optimizer (GWO), and PSO in chaotic regimes. Complementarily, Pérez-Cruz et al. employed hybrid DE/CS/harmony search (HS) optimization for controller synchronization in a new chaotic system, illustrating how metaheuristics extend beyond estimation into control design[11].

Control-oriented applications are particularly relevant. Dali et al. showed that PSO-tuned controllers in Lorenz achieve robust tracking under parameter perturbations and noise[12]. Yau and Chen earlier stressed practical nonlinearities like input saturation, motivating the shift toward optimization-assisted adaptive control[13]. More generally, reviews confirm that swarm and evolutionary algorithms (including GA, DE, PSO, ABC, GWO, FPA, WOA, and others) consistently outperform deterministic baselines for nonlinear and chaotic system identification[14]. Fractional-order and financial chaotic systems have also served as testbeds: Gupta et al. benchmarked ABC, WOA, GWO, and ant colony optimization (ACO), confirming the robustness of nature-inspired search even under fractional dynamics[15].

Recent comparative studies reinforce the growing trend toward hybridization and the incorporation of quantum or chaotic enhancements in parameter identification methods. Approaches such as return-map cost design[2], HEQPSO[4], ACS–PSO[5], ILCOA[6], cellular WOA/SCA[7], GFPA[8], and QFOA[9] have consistently demonstrated superior convergence, reliability, and robustness on Lorenz, Chen, and Rössler benchmarks compared to canonical GA, PSO, and DE. In addition to those advancements, some studies have also demonstrated that chaos-induced optimization frameworks can substantially improve parameter identification accuracy in nonlinear dynamical systems. For example, Mehmood et al.[16] proposed a chaotic aquila optimizer (CAO) by embedding ten chaotic maps to enhance the exploration–exploitation capability of aquila optimizer for electro-hydraulic control system modeling. Similarly, another recent study introduced a chaotic Young's double-slit experiment (CYDSE) optimizer[17], showing that integrating chaotic behavior within physics-based heuristics yields highly accurate identification of nonlinear muscle models. Nevertheless, two limitations remain evident: populations may still collapse prematurely around suboptimal basins, and step-size adaptation often proves inadequate when the error surface exhibits variable curvature across different phases of the search. To address these challenges, the present study introduces a novel framework in which birds of prey-based optimization (BPBO) serves as the behavioral backbone (owing to its four complementary phases of individual hunting, group hunting, attacking the weakest, and relocation) while differential evolution (DE) operators are embedded directly into the update cycle. The resulting hybrid, termed h-BPBODE, applies DE mutation and binomial crossover after each phase-wise candidate update, thereby injecting recombinative diversity while retaining BPBO's adaptive and collective dynamics. In this design, every behavioral move is refined before acceptance, with boundary constraints enforced throughout, ensuring a more balanced and reliable search process.

Extensive simulations were conducted on three representative chaotic systems (Lorenz, Chen, and Rössler) under a common experimental protocol. Comparative analyses against widely used metaheuristics, including original version of BPBO[18], starfish optimization algorithm[19], hippopotamus optimization[20], particle swarm optimization[21] and differential evolution[22], demonstrated that the proposed h-BPBODE consistently achieved superior accuracy and robustness. In all cases, the method was able to recover the exact parameter triplets with negligible residuals, while maintaining faster convergence and tighter error distributions across independent runs. Boxplots and convergence curves confirmed its stability and precision, parameter-evolution plots illustrated smooth trajectories toward ground-truth values, and statistical tables highlighted its clear advantage over competing methods. Furthermore, cross-study comparisons revealed that h-BPBODE surpassed or matched the best-performing hybrid and chaotic-enhanced algorithms reported in the literature, reinforcing

its reliability across benchmarks. In light of the above discussion, the main contributions of this study can be summarized and justified as follows:

1. A novel hybrid framework is developed, in which the DE mutation and crossover operators are embedded within each behavioral phase of the BPBO. This design ensures that every candidate update undergoes an additional recombinative refinement, effectively enhancing the search capacity while preserving BPBO's adaptive and collective dynamics.
2. A more balanced exploration–exploitation mechanism is achieved through this integration. The DE-based perturbations maintain population diversity and prevent premature convergence, while BPBO's cooperative phases intensify the search around promising regions. This dual mechanism directly addresses one of the main shortcomings of conventional metaheuristics in chaotic parameter identification.
3. Extensive validation is performed on three canonical chaotic systems (Lorenz, Chen, and Rössler) that represent distinct levels of dynamical complexity. The consistent accuracy and robustness observed across these cases confirm the algorithm's generalization ability and reliability when applied to nonlinear dynamical problems of varying structure.
4. Cross-benchmark and cross-study competitiveness is established through comparative analyses against both well-known algorithms (e.g., PSO, DE) and recently proposed metaheuristics (e.g., SFOA, HOA). The proposed h-BPBODE not only attains exact parameter recovery at machine precision but also outperforms or matches advanced hybrid and chaos-enhanced approaches previously reported in the literature, thereby reinforcing its methodological relevance and novelty.

The remainder of this paper is organized as follows. Section "Birds of prey-based optimization" reviews the principles of BPBO, outlining its behavioral phases. Section "Hybrid birds of prey-based optimization with differential evolution" presents the proposed hybrid method, h-BPBODE, and details the integration of DE operators into the BPBO update cycle. Section "Problem definition" formulates the parameter-identification problem and summarizes the benchmark systems considered. Section "Simulation results" reports simulation results, comparing h-BPBODE with alternative algorithms and interpreting its performance across Lorenz, Chen, and Rössler systems. Finally, Section "Conclusion" concludes the paper and highlights potential directions for future research.

Birds of prey-based optimization

Birds of prey-based optimization (BPBO) models four observed behaviors of raptors (self-adaptation (individual hunting), cooperative hunting, competition with weaker birds, and continued search when prey is absent) and maps them to exploration–exploitation operators in a single population-based optimizer[18]. In each iteration, the current best solution is treated as the "prey" and the remaining members act as hunters that update their positions via the following phases; the phases may occur stochastically.

Initialization

The initialization generates an initial population of N in D-dimensional hunters within box bounds $[X_{min}, X_{max}]$. For each $i = 1, \ldots, N$:

$$X_i = X_{min} + rand(1, D) \times (X_{max} - X_{min}) \tag{1}$$

where $rand(1, D)$ is a row vector of uniform random numbers in [0,1]. The best member defines the prey (X_{prey}). BPBO has one user parameter P_i ("finding factor") that tunes the exploration–exploitation equilibrium; higher values intensify local refinement, while lower values emphasize global search. In reported experiments, $P_i \approx 0.7$ provided a robust balance across diverse landscapes.

Phase 1: self-adaptation (individual hunting)

In phase one, each hunter adapts its path relative to the prey using:

$$X_i^{new} = X_i + rand(1, D) \times (X_{prey} - K_{i1} X_i), \quad K_{i1} \in \{1,2\} \tag{2}$$

where K_{i1} decides whether the attack is "from behind" ($K_{i1} = 1$) or "from the front" ($K_{i1} = 2$).

Phase 2: cooperative hunting (group search/assault)

Hunters also coordinate around the population center $X_{mean} = \frac{1}{N}\sum_j X_j$. This is defined by phase 2 using Eq. (3).

$$X_i^{new} = X_{mean} + rand(1, D) \times (X_{prey} - K_{i2} X_{mean}), \quad K_{i2} \in \{1,2\} \tag{3}$$

As in Phase 1, K_{i2} toggles front/behind attack directions.

Phase 3: competition (attacking the weakest)

Hunters may opportunistically target the weakest member X_{worst}. This is mimicked via Eq. (4).

$$X_i^{new} = X_i + rand(1, D) \times (X_i - K_{i3} X_i), \quad K_{i3} \in \{1,2\} \tag{4}$$

Here, K_{i3} again encodes front/behind engagement. This phase helps avoid stagnation and exploits easy opportunities.

Phase 4: continued search (relocation)

If a hunter fails to improve, it relocates to explore another region using Eq. (5):

$$X_i^{new} = X_i + rand1 \cdot (X_{min} + rand(1, D) \times (X_{max} - X_{min}) \tag{5}$$

with $rand1 \sim U\,[0,1]$. Basically, after each phase, constraints are enforced on X_i^{new}, and the objective is evaluated. In case ofa better solution is found, X_{prey} is updated. The four phases are invoked randomly during iterations, echoing the varied life-cycle events of raptors. The pseudocode of the BPBO is provided in Algorithm 1.

Hybrid birds of prey-based optimization with differential evolution

The BPBO has shown competitive performance across a wide range of optimization problems. Nevertheless, like many nature-inspired methods, it can occasionally suffer from premature convergence or stagnation in local optima, particularly when solving highly complex landscapes. To enhance its balance between exploration and exploitation, a hybrid strategy is proposed in which differential evolution (DE)[23] operators are integrated directly into the update process of BPBO. The resulting algorithm, termed h-BPBODE, retains the original four behavioral phases of BPBO while enriching each phase with DE's mutation and crossover mechanism to reinforce diversity and intensify local search.

```
Input:
    - Objective function
    - Population size (number of birds)
    - Maximum number of iterations
    - Search space boundaries
Output:
    - Best solution (prey)
Begin
    Generate initial population using Eq. (1)
    Evaluate fitness of all birds
    Identify best solution (prey), worst solution, and average position
    for iteration = 1 to maximum number of iterations do
        for each bird in the population do
            Select a hunting strategy at random:
                if strategy = Individual hunting then
                    Update position using Eq. (2)
                else if strategy = Group hunting then
                    Update position using Eq. (3)
                else if strategy = Attack weakest then
                    Update position using Eq. (4)
                else if strategy = Relocation then
                    Update position using Eq. (5)
                end if
            Apply boundary control
            Evaluate new fitness
            if new fitness is better than old then
                Accept new position
                if new fitness is better than current best then
                    Update best solution (prey)
                end if
            else
                Keep old position
            end if
        end for
    end for
    Return best solution (prey)
End
```

Algorithm 1. Pseudocode of the BPBO.

Differential evolution operators

In the hybrid design, two classical operators from DE are employed (mutation and binomial crossover). In case of mutation, is generated as in Eq. (6) for a current candidate solution, a mutant vector:

$$V_i = X_i + F \cdot (X_{r1} - X_{r2}) \tag{6}$$

where X_i is the current bird, X_{r1} and X_{r2} are two distinct randomly chosen individuals from the population, and $F \in [0,2]$ is the scaling factor that regulates the step size. The mutant vector is then recombined with the current bird to form a trial vector in case of binomial crossover given in Eq. (7):

$$U_{i,j} = \begin{cases} V_{i,j}; & rand_j \leq CR \, or \; : j = j_{rand} \\ X_{i,j}; & otherwise \end{cases} \tag{7}$$

where $CR \in [0,1]$ denotes the crossover probability, $rand_j$ is a random number in [0,1] and j_{rand} ensures that at least one dimension is inherited from the mutant. The trial solution replaces the parent if it provides a superior fitness.

Embedding strategy within BPBO

The hybrid algorithm preserves the four canonical phases of BPBO—individual hunting, group hunting, attack-the-weakest, and relocation. For each bird in the population, one of these phases is selected as in the original framework. After the phase generates a new candidate position, the DE mutation and crossover operators (Eqs. 6 and 7) are immediately applied to refine this candidate. The resulting trial solution is then evaluated and accepted only if it improves the fitness value. This procedure guarantees that every behavioral move of BPBO is enhanced by an additional DE-based refinement, thereby combining the exploratory ability of BPBO with the recombinative search of DE. Specifically:

- In the individual hunting phase, the move toward the prey (Eq. 2) is followed by DE refinement.
- In the group hunting phase, the candidate based on the mean position (Eq. 3) is refined by DE.
- In the attack-the-weakest phase, the opportunistic move against the worst member (Eq. 4) is refined by DE.
- In the relocation phase, the random exploratory move (Eq. 5) is refined by DE.

In all cases, boundary constraints are enforced after refinement, and the best solution (prey) is updated if a superior candidate is discovered. The integration of DE within BPBO ensures that every update is accompanied by a recombinative refinement step, which enhances both the exploration capacity and the convergence speed. The additional computational cost is modest, as the hybrid requires only one extra trial evaluation per bird at each iteration. As a result, h-BPBODE offers a more robust search process than the original BPBO while maintaining similar computational complexity. Figure 1. illustrates a detailed flowchart of proposed h-BPBODE.

Time complexity of h-BPBODE

The computational cost of the proposed h-BPBODE algorithm is governed by several parameters: the number of search agents (N), the dimensionality of the optimization problem (D), the maximum number of iterations ($Iter_{max}$), and the average cost of a single objective-function evaluation (C). The overall time complexity of the original BPBO can be expressed as the sum of four major components: parameter initialization, population initialization, fitness evaluation, and population update:

$$\begin{aligned} O\,(BPBO) = {} & O(parameter_setup) + O(population_initialization) \\ & + O(function_evaluations) + O(population_updates) \end{aligned} \tag{8}$$

Each component can be quantified as follows:

- Parameter setup: $O\,(1)$, since it involves assigning initial control constants.
- Population initialization: $O(N \times D)$, corresponding to the random generation of initial candidate solutions.
- Function evaluations: $O(N \times C \times Iter_{max})$, representing the dominant cost due to repeated fitness computations.
- Population updates: $\mathrm{O}(N \times D \times Iter_{\max})$, accounting for iterative position and velocity updates.

Hence, the total computational complexity of BPBO is:

$$\begin{aligned} O\,(BPBO) &= O\,(1) + O(N \times D) + O(N \times C \times Iter_{max}) + O(N \times D \times Iter_{max}) \\ &\approx O(N \times (C + D) \times Iter_{max}) \end{aligned} \tag{9}$$

In the proposed hybrid version, DE operators are embedded within each behavioral phase of BPBO.

The DE component introduces additional mutation and crossover operations as well as function evaluations for the newly generated trial solutions. Their respective complexities are:

$$O(N \times C \times Iter_{max}) \tag{10}$$

Therefore, the total complexity of DE can be approximated by:

$$O\,(DE) = O(N \times Iter_{max} \times (C + D\,)) \tag{11}$$

When DE is coupled with BPBO, the cumulative complexity of the hybrid algorithm becomes:

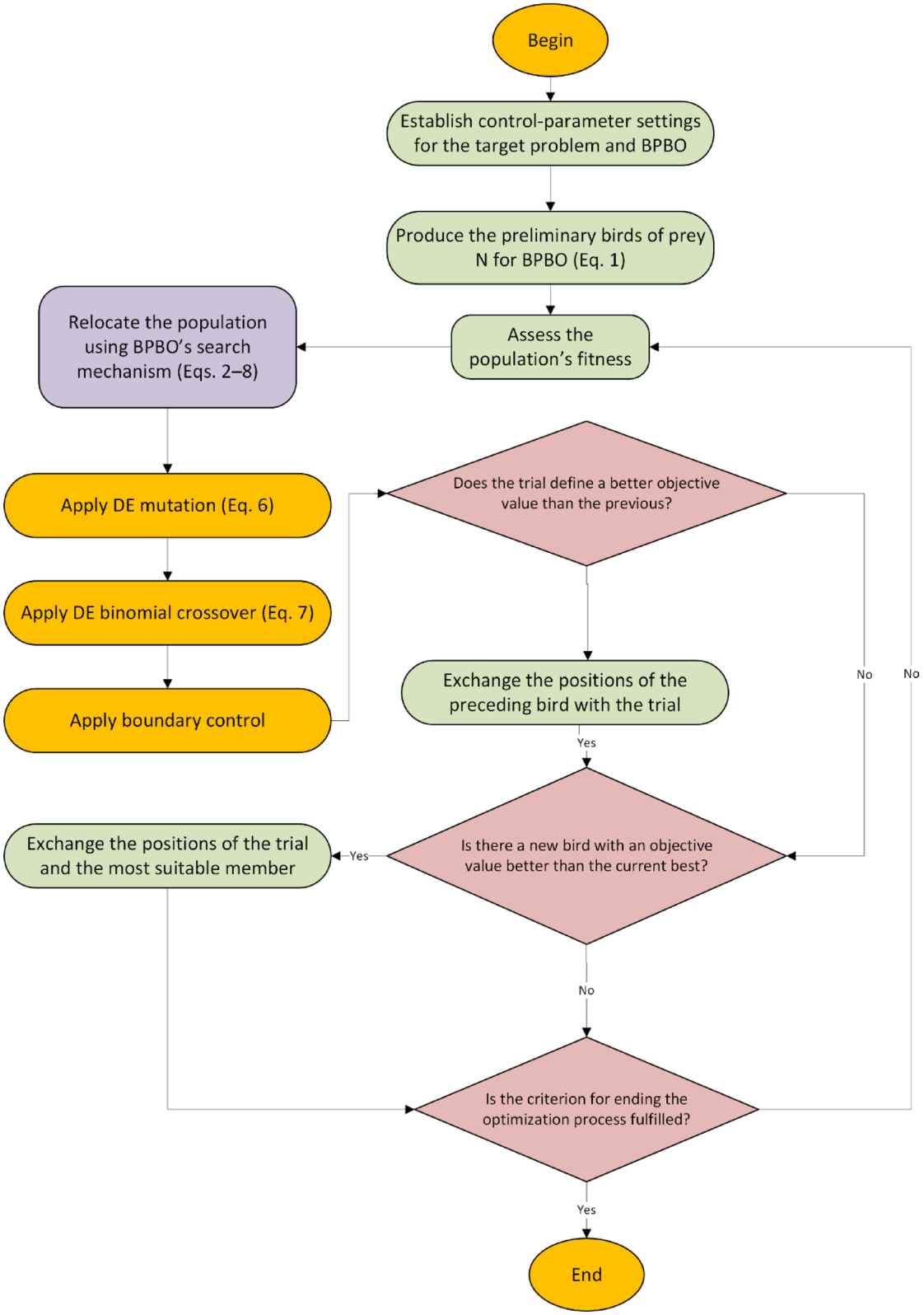


Fig. 1. Flowchart of proposed h-BPBODE.

$$\begin{aligned} O\left(\mathrm{h}-\mathrm{BPBODE}\right) &= O\left(N \times (C+D) \times Iter_{max}\right) + O\left(N \times Iter_{max} \times (C+D)\right) \\ &= O\left(2 \times N \times (C+D) \times Iter_{max}\right) \end{aligned} \tag{12}$$

Asymptotically, this expression indicates that the proposed h-BPBODE preserves the same order of growth as BPBO and DE. The additional factor of two arises from the embedded recombination operations but does not alter the Big-O order. Consequently, the hybrid algorithm achieves enhanced convergence accuracy and stability without a significant increase in computational complexity.

Problem definition

Accurate parameter identification is a critical requirement for chaotic systems, since even small variations in system parameters can produce fundamentally different trajectories[6–8]. In this work, the parameter estimation problem is treated as an optimization task in which the goal is to minimize the error between the observed trajectory of the true system and the trajectory generated by a simulated model with candidate parameters. Let the reference system be denoted as:

$$\dot{X} = F(X, \theta_0) \tag{13}$$

where $X = [x, y, z]$ represents the system states and $\theta_0 = [\mathrm{a}, \mathrm{b}, \mathrm{c}]$ are the actual parameters. Using the same initial conditions, a simulated model is written as:

$$\dot{\tilde{X}} = F(\tilde{X}, \theta) \tag{14}$$

with θ being the estimated parameter vector. The objective of identification is then formulated as:

$$Mean\,squared\,error\ (MSE) = J(\theta) = \frac{1}{M}\sum_{k=1}^{M}\left\|X_k - \tilde{X}_k(\theta)\right\|^2 \tag{15}$$

where M is the number of sampled data points. The optimization problem is therefore expressed as finding $\theta^* = \underset{\theta\in\Omega}{\operatorname{argmin}} J(\theta)$ with Ω denoting the feasible parameter space defined for each system.

In this study, three representative chaotic systems are adopted as benchmarks: Lorenz, Chen, and Rössler, whose mathematical models, parameter ranges, and actual parameters are summarized in Table 1. These systems have been widely used in the literature for evaluating identification algorithms because of their distinctive properties:

- Lorenz system[24] was originally introduced as a simplified model of atmospheric convection, it is the most classical chaotic benchmark. Its butterfly-shaped attractor illustrates strong sensitivity to initial conditions and parameter changes, making it a standard test for parameter estimation[25].
- Although Chen system is structurally related to Lorenz, it is not topologically equivalent and demonstrates more intricate chaotic dynamics[26]. It is often used to evaluate the robustness of identification methods when facing stronger nonlinearities and richer attractor behaviors.
- Rössler system is a relatively simple three-dimensional oscillator with only one nonlinear term[27]. It produces spiral-type chaotic attractors and offers a complementary test case that is less structurally complex but still exhibits chaotic dynamics.

By including these three systems, the identification task spans different types of chaotic dynamics, from the well-known Lorenz attractor to the more complex Chen system and the structurally simpler Rössler oscillator. This ensures that the proposed algorithm is validated against systems with varying levels of dynamical richness and identification difficulty. Figure 2 provides a flowchart demonstrating the application of the proposed optimizer for estimating the parameters of the chaotic systems investigated in this study.

System type	Model equations	Parameter range	Actual model parameters
Lorenz chaotic system	$\dot{x} = a(y - x)$	$0 \le a \le 20$	$a = 10$
	$\dot{y} = bx - xz - y$	$0 \le b \le 50$	$b = 28$
	$\dot{z} = xy - cz$	$0 \le c \le 5$	$c = 8/3$
Chen chaotic system	$\dot{x} = a(y - x)$	$20 \le a \le 50$	$a = 35$
	$\dot{y} = (c - a)x - cy - xz$	$1 \le b \le 6$	$b = 3$
	$\dot{z} = xy - bz$	$10 \le c \le 40$	$c = 28$
Rössler chaotic system	$\dot{x} = -y - z$	$0 \le a \le 1$	$a = 0.2$
	$\dot{y} = x + ay$	$0 \le b \le 1$	$b = 0.2$
	$\dot{z} = b + (x - c)z$	$0 \le c \le 10$	$c = 5.7$

Table 1. Model equations, parameter ranges and actual model parameters of the systems adopted for this study.

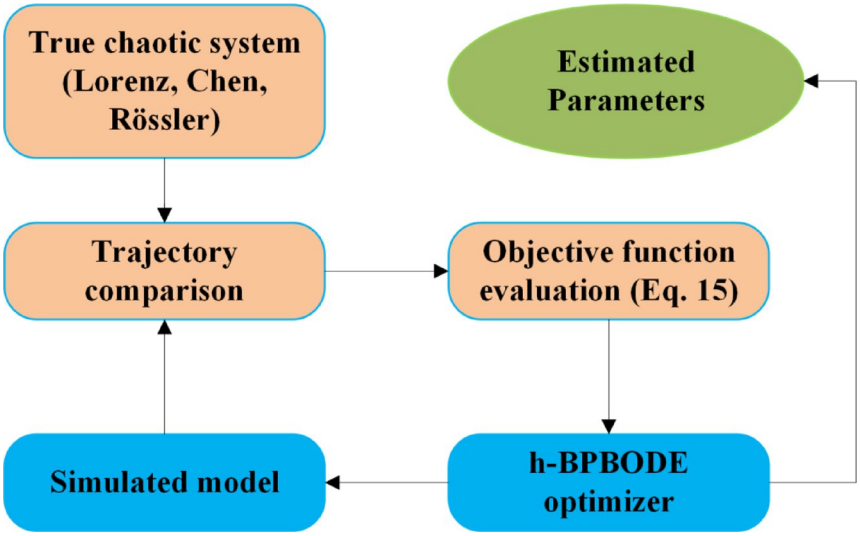


Fig. 2. The application of h-BPBODE for parameter estimation of chaotic systems.

Simulation results

This section reports the identification performance of the proposed h-BPBODE on three benchmark chaotic systems (Lorenz, Chen, and Rössler) under a common protocol (25 independent runs, population size = 30, 500 iterations). Comparisons are made against the original version of BPBO[18], starfish optimization algorithm (SFOA)[19], hippopotamus optimization (HO)[20], particle swarm optimization (PSO)[21] and differential evolution (DE)[22]. For each system, results are presented as (i) boxplots of objective values, (ii) descriptive statistics (minimum, maximum, median, mean, standard deviation), (iii) convergence curves, (iv) parameter-evolution traces for a, b, and c, and (v) final parameter tables; additional cross-study tables summarize comparisons with methods reported in prior literature. This layout enables a like-for-like assessment of accuracy, stability, and convergence speed across algorithms and systems. The simulations were performed on the Lorenz, Chen, and Rössler systems, whose mathematical models, parameter ranges, and actual parameter values are summarized in Table 1. These ground-truth settings serve as the reference for evaluating the accuracy of the estimated parameters reported in subsequent tables and figures.

It is worth emphasizing that the comparative framework employed in this study encompasses both recently introduced algorithms, such as the SFOA[19], HO[20], and widely established baselines, including PSO[21] and DE[22]. This dual inclusion enables a balanced evaluation across algorithmic generations, demonstrating that the proposed hybrid h-BPBODE maintains superiority not only over emerging metaheuristics but also over reference methods that continue to serve as standard benchmarks in contemporary optimization research. In addition, the investigation contributes to an area where metaheuristic applications remain relatively limited (chaotic parameter identification) thereby reinforcing the relevance of the comparative design adopted in this work.

It should also be noted that the proposed hybrid framework was evaluated alongside its constituent algorithms (namely, the original BPBO and the classical DE) under identical experimental settings. This inclusion provides an ablation-style validation, allowing the isolated effect of DE operators on BPBO's performance to be observed directly. The results presented in the statistical tables and boxplots consistently reveal that h-BPBODE attains lower variance, faster convergence, and smaller mean error compared to both BPBO and DE alone. These findings substantiate that the embedded mutation and crossover operations effectively enhance BPBO's exploration–exploitation balance by maintaining population diversity while reinforcing convergence toward the optimal region. Moreover, the comparative set includes not only classical benchmarks such as PSO and DE but also recently developed metaheuristics like SFOA and HOA, thereby ensuring a fair and up-to-date evaluation across algorithmic generations.

Lorenz system

The Lorenz benchmark was first used to examine whether the proposed h-BPBODE can recover parameters with both high accuracy and run-to-run stability under the common protocol (25 runs, population size 30, 500 iterations). Performance is summarized through a boxplot of objective values, descriptive statistics, convergence traces of the objective, parameter-evolution plots for a, b, and c, and the final parameter estimates with residuals. A literature comparison is also provided.

A highly concentrated box with virtually no visible upper whisker is observed for h-BPBODE in Fig. 3, consistent with Table 2, where the minimum, median, and maximum objective values are reported as 0, 0, and 1.8932E−28, respectively, yielding an average of 2.1000E−29 and a standard deviation of 4.6732E−29. In contrast, the competing methods show broader dispersion and clearly higher centers: BPBO (mean 9.4169E−10, standard deviation 4.6039E−09), SFOA (mean 4.4547E−14), HO (mean 5.1379E−08), PSO (mean 2.8208E−06),

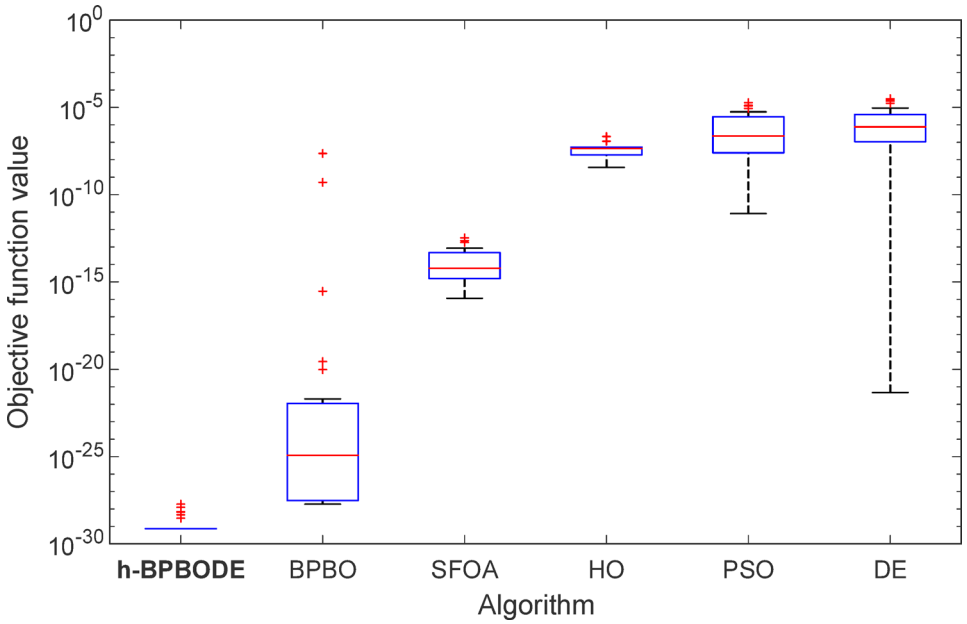


Fig. 3. Comparative boxplots corresponding to the objective function values for Lorenz system.

Algorithm	Minimum	Maximum	Median	Average	Standard Deviation
h-BPBODE	**0**	**1.8932E−28**	**0**	**2.1000E−29**	**4.6732E−29**
BPBO	1.8932E−28	2.3035E−08	1.2095E−25	9.4169E−10	4.6039E−09
SFOA	1.1487E−16	3.3162E−13	6.1019E−15	4.4547E−14	8.2815E−14
HO	3.6594E−09	2.1463E−07	4.3373E−08	5.1379E−08	4.9105E−08
PSO	8.1632E−12	1.8648E−05	2.2822E−07	2.8208E−06	5.0690E−06
DE	4.7049E−22	3.1386E−05	7.6728E−07	5.2217E−06	9.1168E−06

Table 2. Comparative statistical results for Lorenz system. Significant values are in bold.

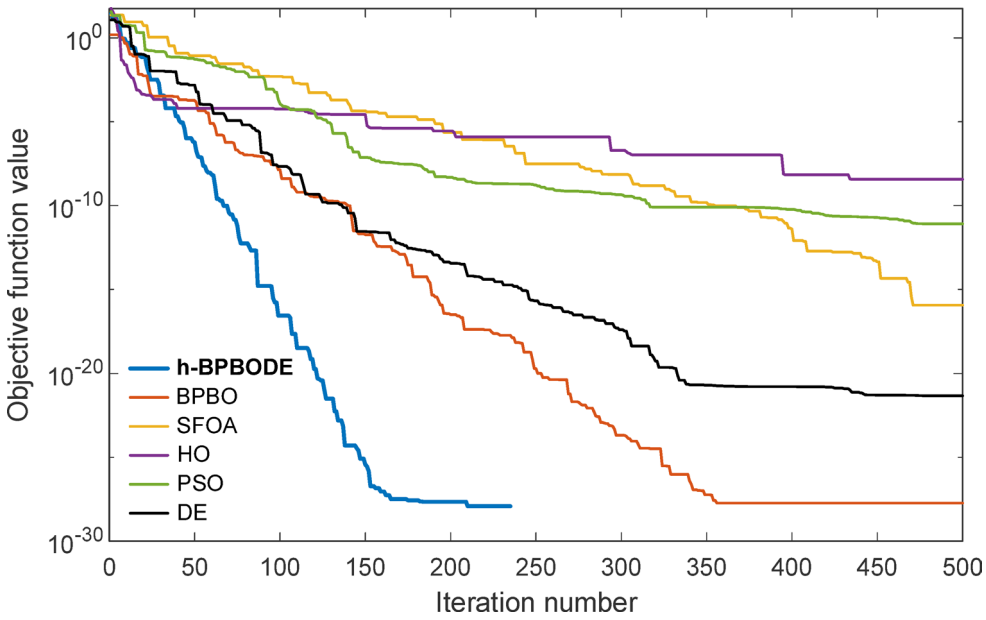


Fig. 4. Convergence of objective function for Lorenz system using different approaches.

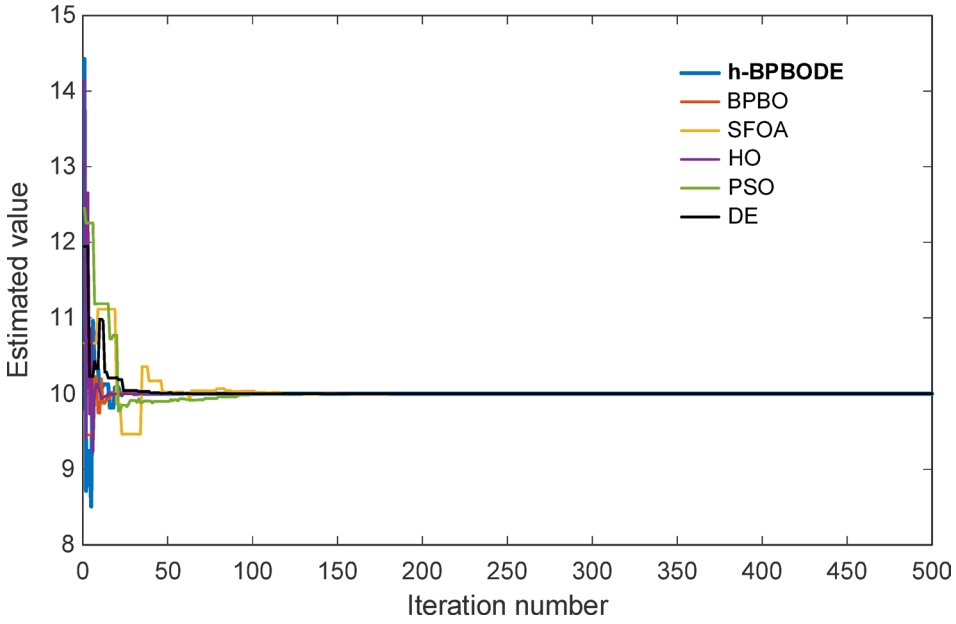


Fig. 5. Evolution of parameter a for Lorenz system.

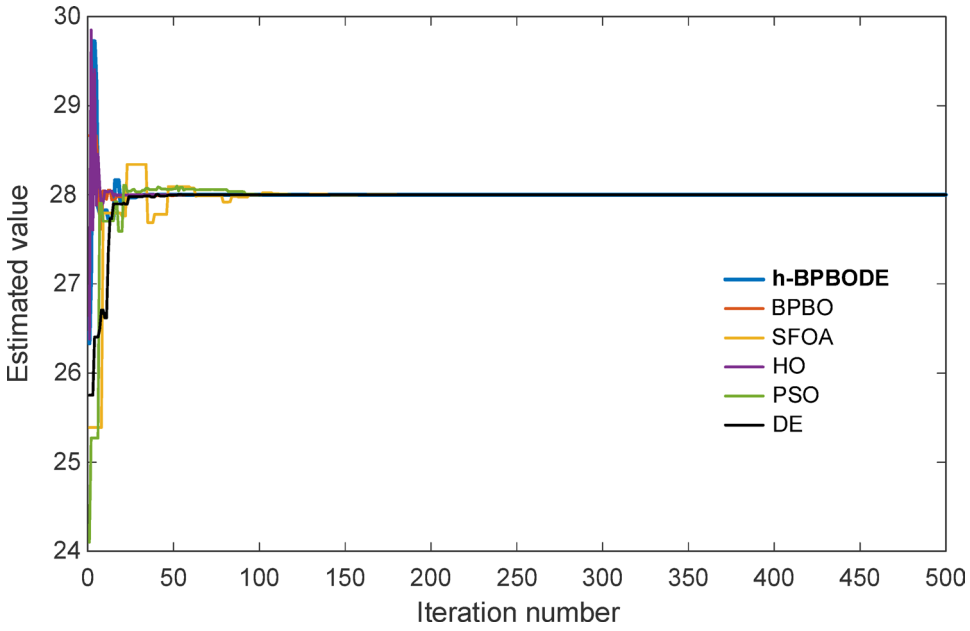


Fig. 6. Evolution of parameter b for Lorenz system.

and DE (mean 5.2217E−06). These summaries indicate that h-BPBODE consistently lands at (or numerically indistinguishable from) the global optimum, while the alternatives retain noticeable residuals across runs.

In terms of convergence behavior (Fig. 4), the objective for h-BPBODE descends rapidly and stabilizes at machine-precision levels well before the iteration budget is exhausted. The remaining approaches show slower decay and higher terminal plateaus, which aligns with their larger averages and upper tails in Table 2. This behavior suggests that embedding DE refinement within the BPBO update contributes to faster approach to the optimum without sacrificing stability.

The parameter trajectories for Lorenz system are provided in Figs. 5, 6 and 7. The evolution curves for a, b, and c exhibit smooth, monotone-like convergence towards the true Lorenz parameters. According to Table 3, h-BPBODE recovers the exact triplet within the reported precision ($a = 10.000000$, $b = 28.000000$, $c = 2.666667$) with a final objective of 0. BPBO and DE also reach the exact triplet numerically but retain tiny residuals (1.8932E−28 and 4.7049E−22, respectively), whereas SFOA, HO, and PSO display either parameter-

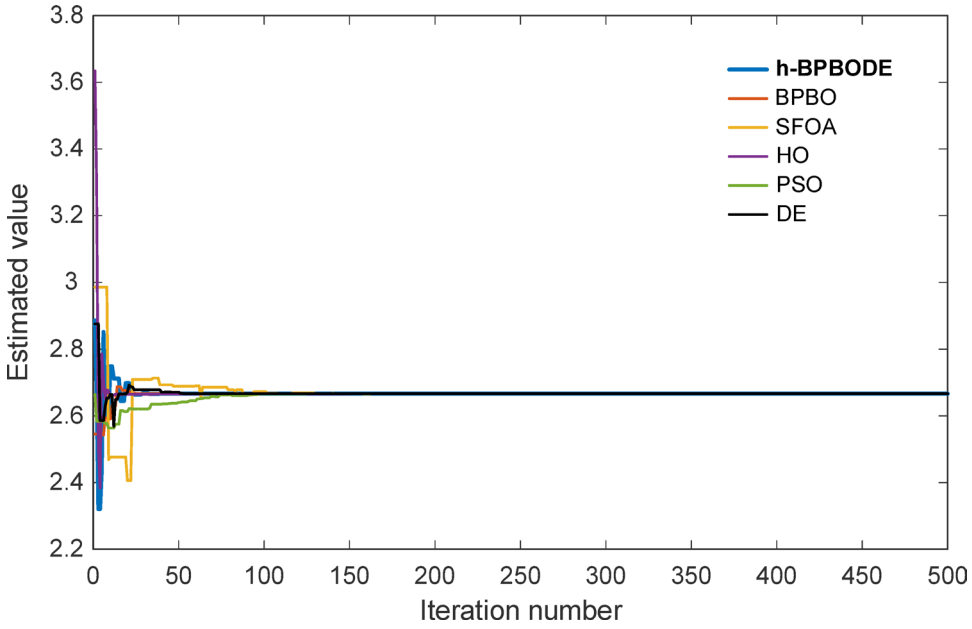


Fig. 7. Evolution of parameter c for Lorenz system.

Algorithm	a	b	c	MSE
h-BPBODE	10.000000	28.000000	2.666667	**0**
BPBO	10.000000	28.000000	2.666667	1.8932E−28
SFOA	10.000000	28.000000	2.666667	1.1487E−16
HO	10.000036	27.999967	2.666672	3.6594E−09
PSO	9.999999	28.000002	2.666666	8.1632E−12
DE	10.000000	28.000000	2.666667	4.7049E−22

Table 3. Parameters and MSE values obtained from different approaches for Lorenz system. Significant values are in bold.

Algorithm	a	b	c	MSE
h-BPBODE	10.000000	28.000000	2.666667	**0**
QFOA	10.00	28.00	2.6666	9.53E−09
CS	10.00	28.00	2.6664	1.71E−04
GA	10.027	28.01	2.6691	1.332

Table 4. Comparative obtained parameters and MSE values with respect to reported approaches for Lorenz system. Significant values are in bold.

level deviations, nonzero residuals, or both. These findings are consistent with the tighter distribution seen in Fig. 3.

Comparison with reported approaches for Lorenz system are presented in Table 4. In this regard, quantum fruit fly optimization algorithm (QFOA)[9], cuckoo search (CS) algorithm[9] and genetic algorithm (GA)[9] are adopted for comparison. When contrasted with representative methods from the literature, the proposed h-BPBODE attains zero objective while exactly matching the ground-truth parameters, outperforming previously reported residuals (e.g., 9.53E − 09 for QFOA, 1.71E − 04 for CS, and 1.332 for GA). This result further underlines the robustness of the hybrid strategy for Lorenz parameter identification. Across distributional statistics, convergence speed, trajectory smoothness, and final accuracy, h-BPBODE demonstrates a decisive advantage on the Lorenz system. The near-zero dispersion and exact recovery reported in Tables 2 and 3; Fig. 3 signify that the hybrid update effectively mitigates premature convergence and locks onto the correct parameter set with high reliability.

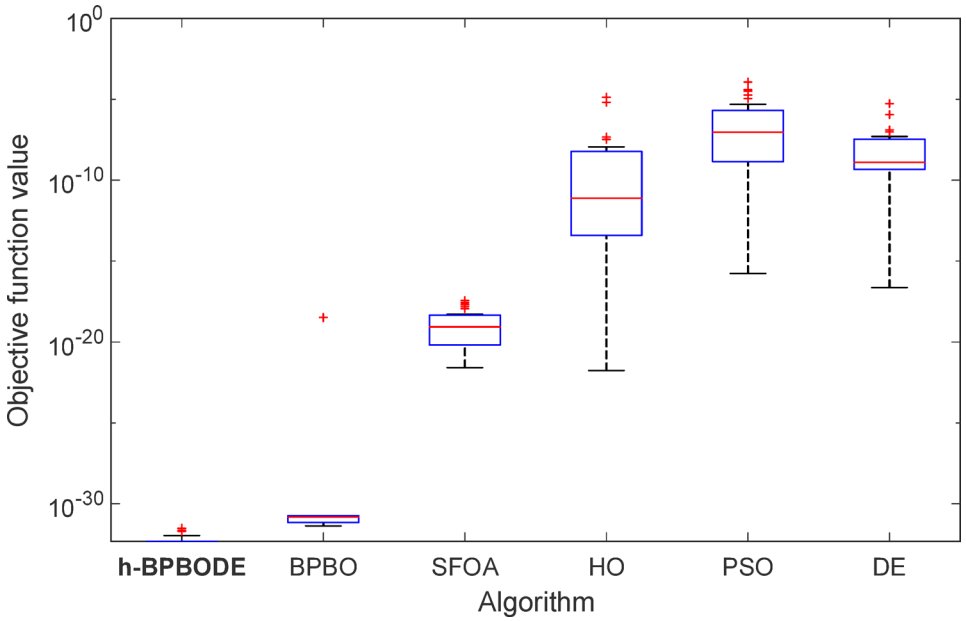


Fig. 8. Comparative boxplots corresponding to the objective function values for Chen system.

Algorithm	Minimum	Maximum	Median	Average	Standard Deviation
h-BPBODE	**0**	**3.0957E−32**	**0**	**5.1046E−33**	**9.6463E−33**
BPBO	4.3002E−32	3.2357E−19	1.4875E−31	6.4714E−20	1.3210E−19
SFOA	2.6644E−22	3.5908E−18	8.8449E−20	5.3229E−19	9.5222E−19
HO	1.7471E−22	1.3510E−05	7.5610E−12	8.0799E−07	2.9514E−06
PSO	1.7089E−16	1.1695E−04	9.2129E−08	9.0256E−06	2.4765E−05
DE	2.2908E−17	5.4523E−06	1.2636E−09	2.8010E−07	1.1009E−06

Table 5. Comparative statistical results for Chen system. Significant values are in bold.

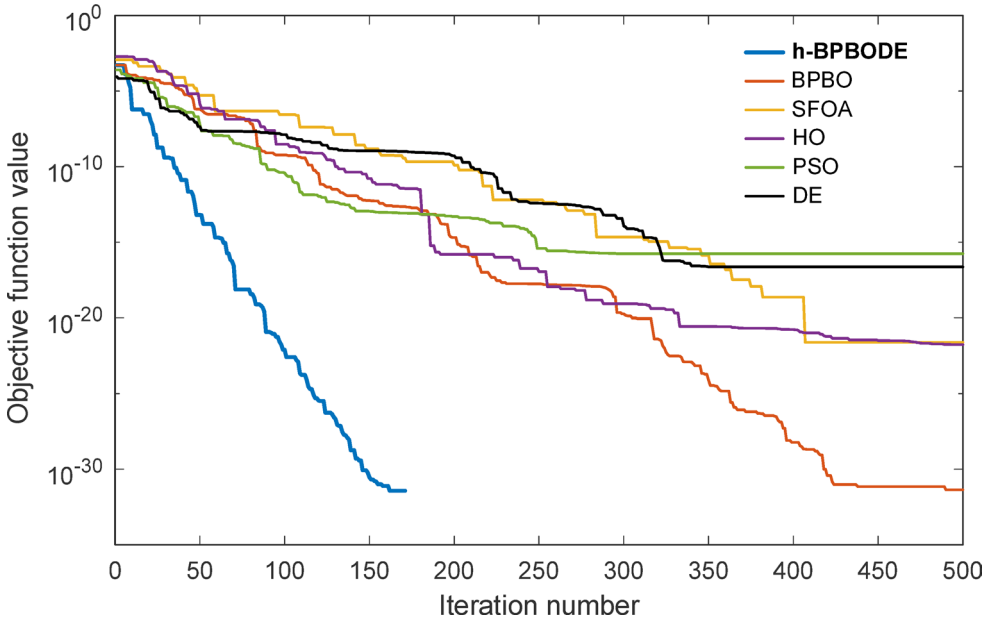


Fig. 9. Convergence of objective function for Chen system using different approaches.

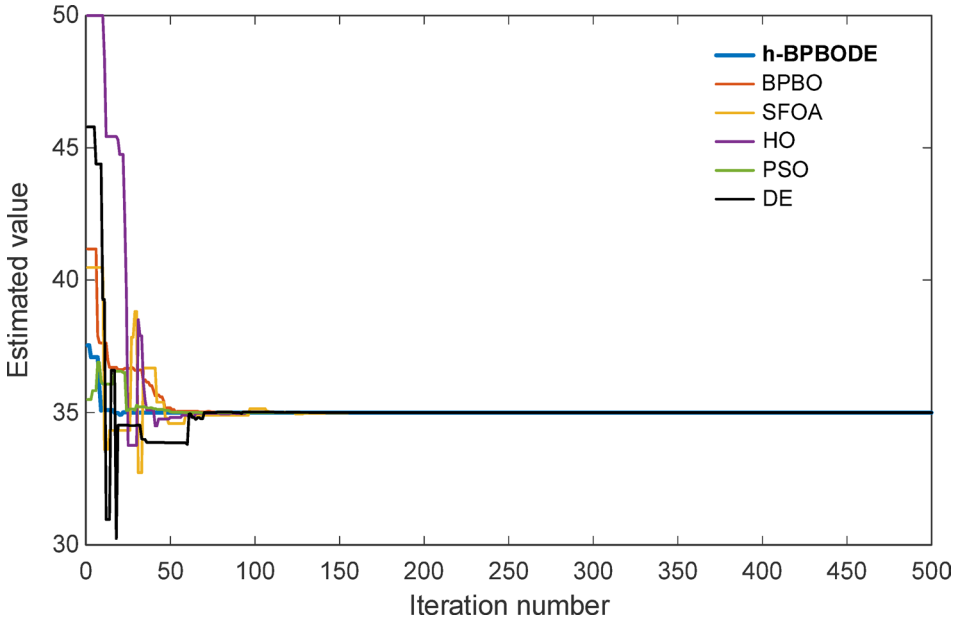


Fig. 10. Evolution of parameter a for Chen system.

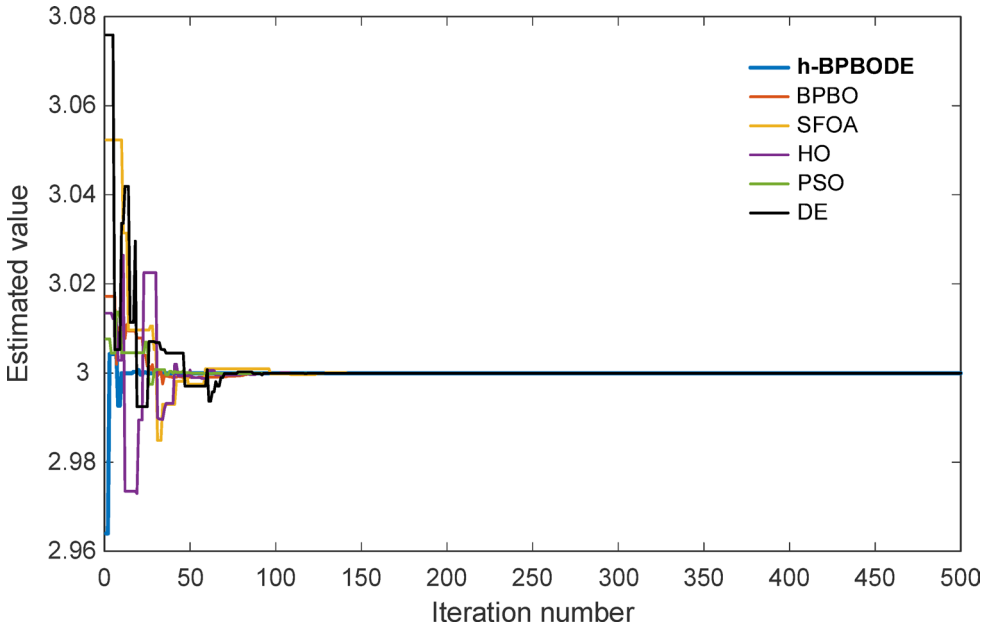


Fig. 11. Evolution of parameter b for Chen system.

Chen system

The Chen benchmark was employed to assess identification performance under a more intricate chaotic regime. Results have been organized as a boxplot of objective values (Fig. 8), a table of descriptive statistics (Table 5), convergence traces of the objective (Fig. 9), parameter-evolution plots for a, b, and c (Figs. 10, 11 and 12), and a table of final parameter estimates with residuals (Table 6). A separate comparison with representative studies from the literature is also provided (Table 7). Together, these materials enable a direct examination of accuracy, stability, and convergence behavior for the proposed and baseline optimizers.

The boxplot (Fig. 8) for the proposed method shows a highly compact distribution centered at zero. This visual impression is confirmed by Table 5, where the minimum, median, and maximum objective values of h-BPBODE are reported as 0, 0, and 3.0957E−32, respectively, with a mean of 5.1046E−33 and standard deviation of 9.6463E−33. In contrast, the competing approaches present substantially broader spreads and higher central tendencies. These statistics indicate that h-BPBODE maintains both a lower central error and a markedly smaller dispersion relative to the alternatives.

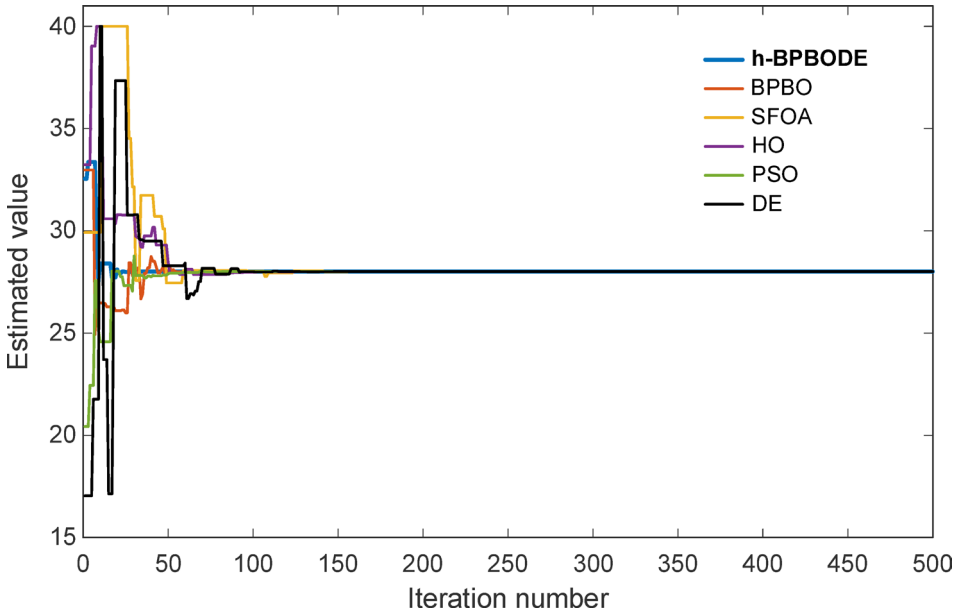


Fig. 12. Evolution of parameter c for Chen system.

Algorithm	a	b	c	MSE
h-BPBODE	35.000000	3.000000	28.000000	**0**
BPBO	35.000000	3.000000	28.000000	4.3002E−32
SFOA	35.000000	3.000000	28.000000	2.6644E−22
HO	35.000000	3.000000	28.000000	1.7471E−22
PSO	35.000000	3.000000	28.000007	1.7089E−16
DE	35.000000	3.000000	27.999997	2.2908E−17

Table 6. Parameters and MSE values obtained from different approaches for Chen system. Significant values are in bold.

Algorithm	a	b	c	MSE
h-BPBODE	35.000000	3.000000	28.000000	**0**
ILCOA	35.0000	3.0000	28.0000	4.2867E−34
ABC	35.4466	2.8680	28.2542	2.1683
WHALE-L5	34.99976	2.99999	27.99732	2.77972E−07

Table 7. Comparative obtained parameters and MSE values with respect to reported approaches for Chen system. Significant values are in bold.

Comparative convergence behavior for Chen system is provided in Fig. 9. The convergence curves show that the hybrid method reaches near-machine-precision objective values early and sustains them throughout the remaining iterations. The baseline algorithms exhibit slower decay and higher terminal plateaus, which is consistent with their larger means and variances in Table 5. This pattern suggests that the embedded DE refinement within BPBO improves the rate and reliability of descent on the Chen landscape.

Parameter trajectories for chen system are provided in Figs. 10, 11 and 12. The evolution plots for a, b, and c display smooth movement toward the true Chen parameters, with minimal oscillation once the vicinity of the solution is reached. As summarized in Table 6, h-BPBODE recovers the exact triplet (35.000000, 3.000000, 28.000000) with a final objective of 0 at the reported precision. BPBO, SFOA, and HO also return the exact parameter triplet numerically, though with nonzero residuals on the order of 10^{-32}–10^{-22}. PSO and DE yield very small but detectable deviations in c (28.000007 and 27.999997, respectively), accompanied by higher residuals (1.7089E−16 and 2.2908E−17). These findings align with the more concentrated distribution observed for h-BPBODE in Fig. 8.

Comparison with reported approaches is also provided for Chen system as shown in Table 7. When contrasted with representative methods from the literature (improved Lozi map based chaotic optimization

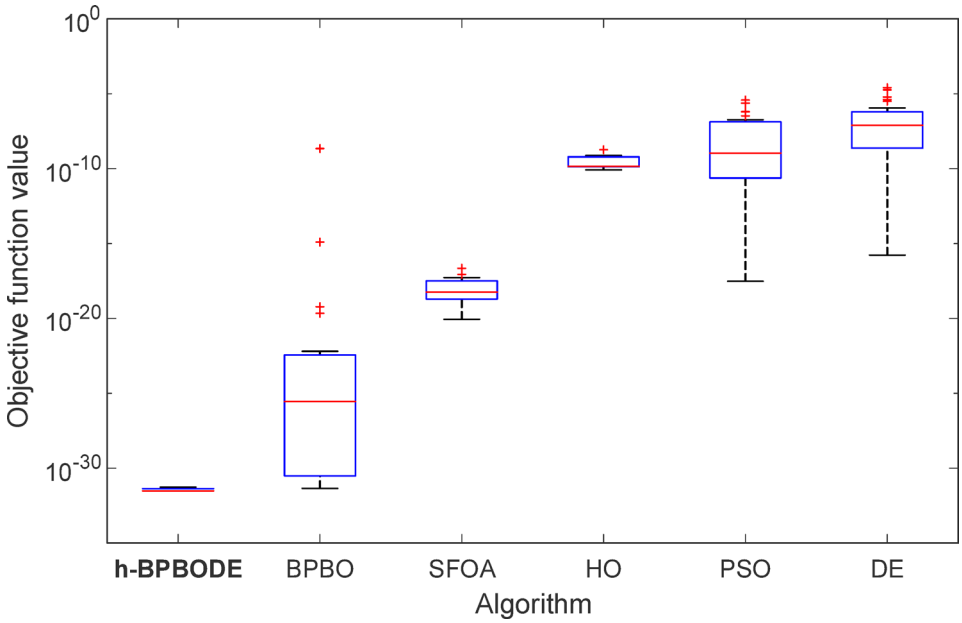


Fig. 13. Comparative boxplots corresponding to the objective function values for Rössler system.

Algorithm	Minimum	Maximum	Median	Average	Standard Deviation
h-BPBODE	**0**	**5.4232E−32**	**2.9986E−32**	**2.3735E−32**	**2.2511E−32**
BPBO	4.4285E−32	2.2189E−09	2.7950E−26	8.8756E−11	4.4378E−10
SFOA	8.6520E−21	2.2324E−17	5.7479E−19	2.4365E−18	4.7004E−18
HO	8.3002E−11	1.8334E−09	1.4557E−10	5.7411E−10	6.7126E−10
PSO	3.0229E−18	3.8221E−06	1.0844E−09	3.3476E−07	8.7705E−07
DE	1.6828E−16	2.5594E−05	7.7731E−08	2.4141E−06	6.1664E−06

Table 8. Comparative statistical results for Rössler system. Significant values are in bold.

algorithm (ILCOA)[6], artificial bee colony (ABC)[6] and cellular whale and sine–cosine algorithm (WHALE-L5)[7]. The proposed approach achieves zero objective while matching the ground-truth parameters, outperforming the nonzero residuals reported for the comparators (e.g., 4.2867E − 34 for ILCOA, 2.1683 for ABC, and 2.77972E − 07 for WHALE-L5). This cross-study comparison indicates that the hybrid strategy remains competitive even against specialized algorithms previously tailored for Chen parameter identification. Across distributional statistics, convergence speed, and final parameter accuracy, the Chen experiments consistently favor h-BPBODE. The combination of near-zero dispersion and exact recovery reported in Table 6 (together with the early and stable convergence in Fig. 9) suggests that the hybrid update effectively maintains diversity while guiding the search toward the correct parameter set with high reliability on this more challenging chaotic system.

Rössler system

The Rössler benchmark was employed to test identification performance on a chaotic oscillator with a single quadratic nonlinearity. The reporting follows the comparative boxplots of the objective values (Fig. 13), descriptive statistics (Table 8), convergence behavior (Fig. 14), parameter-evolution plots for a, b, and c (Figs. 15, 16 and 17), and a table of final parameter estimates with residual error (Table 9). In addition, a cross-study comparison is provided against representative methods from the literature (Table 10).

The boxplot (Fig. 13) for the proposed method exhibits a compact distribution centered near zero. As summarized in Table 8, h-BPBODE achieves a median objective of 2.9986E−32, with minimum 0, maximum 5.4232E−32, average 2.3735E−32, and standard deviation 2.2511E−32. By contrast, the alternatives show broader spreads and markedly higher centers: BPBO (mean 8.8756E−11), SFOA (mean 2.4365E−18), HO (mean 5.7411E−10), PSO (mean 3.3476E−7), and DE (mean 2.4141E−6). These results indicate that h-BPBODE maintains both lower central error and tighter dispersion relative to the baselines on Rössler.

Comparative convergence behavior for Rössler system is provided in Fig. 14. The convergence curves show that the hybrid method descends rapidly to near machine precision and remains stable thereafter, whereas the competing approaches display slower decay and notably higher terminal plateaus. This qualitative gap mirrors the statistics in Table 8, reinforcing that the embedded DE refinement inside BPBO expedites and stabilizes convergence on this problem.

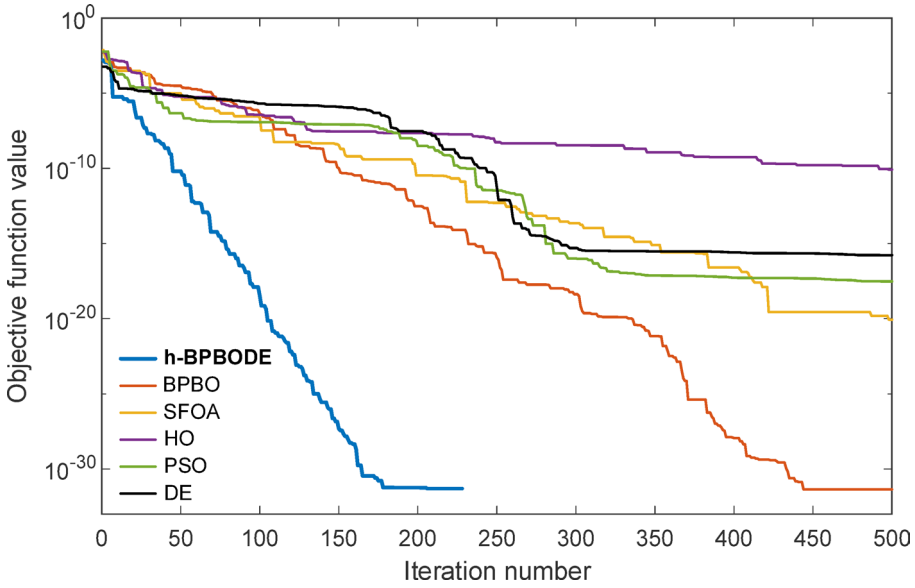


Fig. 14. Convergence of objective function for Rössler system.

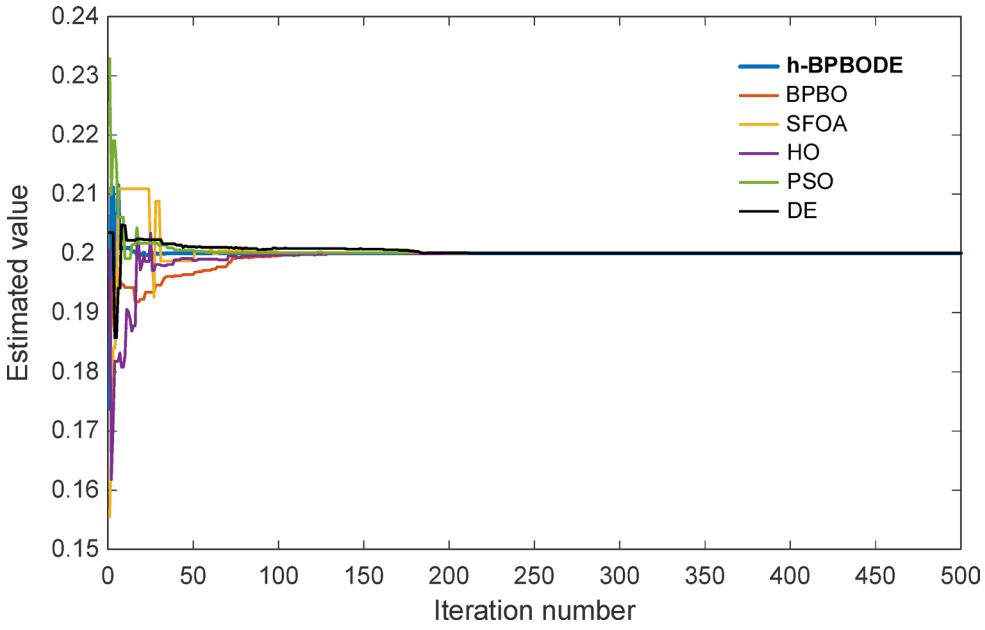


Fig. 15. Evolution of parameter a for Rössler system.

Parameter trajectories for Rössler system are provided in Figs. 15, 16 and 17. The evolution plots for a, b, and c reveal smooth approaches toward the ground-truth parameters. In Table 9, h-BPBODE matches the exact triplet at the reported precision (0.200000, 0.200000, 5.700000) with a final objective of 0. BPBO and several baselines also reach the exact values numerically, yet retain nonzero residuals (e.g., BPBO 4.4285E−32; SFOA 8.6520E−21; PSO 3.0229E−18; DE 1.6828E−16). HO exhibits small deviations in a and b (e.g., 0.199999 and 0.200055) along with a higher residual (8.3002E−11). These outcomes are consistent with the tighter box observed for the hybrid method in Fig. 13.

Comparison with reported approaches for Rössler system is provided in Table 10. Against external references (flower pollination algorithm (FPA)[8], improved fruit fly algorithm (IFFO)[8] and quantum particle swarm optimization (QPSO)[8], the proposed method again returns the exact parameter triplet with zero objective. The literature methods obtain very small residuals (e.g., 4.1654E − 7 for FPA; 2.0942E − 7 for IFFO; 2.1341E − 11 for QPSO) together with parameter values that are close to the ground truth but not exact at the reported precision.

This cross-study view further supports the robustness and accuracy of h-BPBODE on the Rössler identification task. Across the Rössler experiments, the hybrid approach demonstrates fast and stable convergence, near-zero

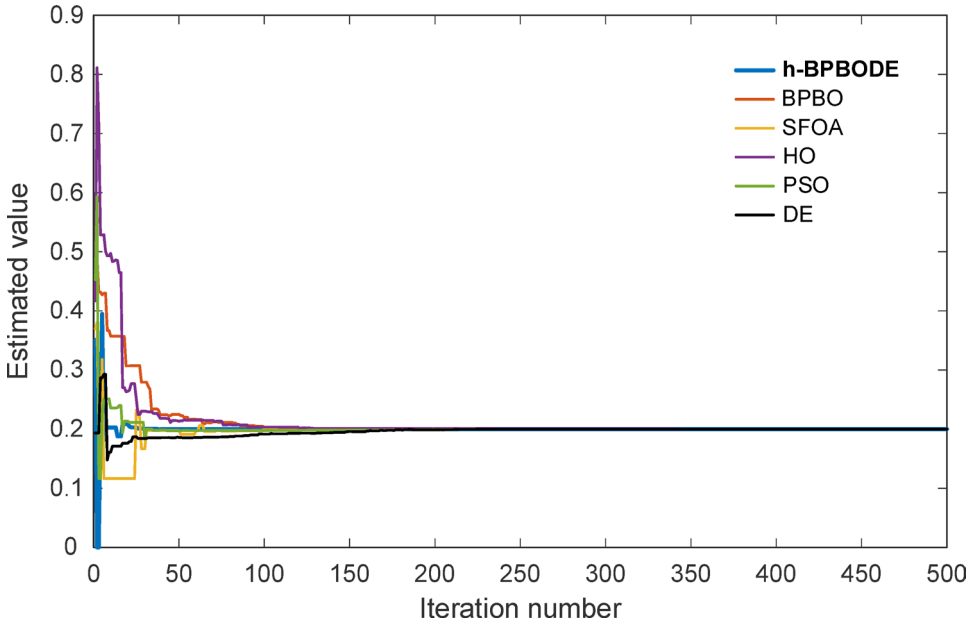


Fig. 16. Evolution of parameter b for Rössler system.

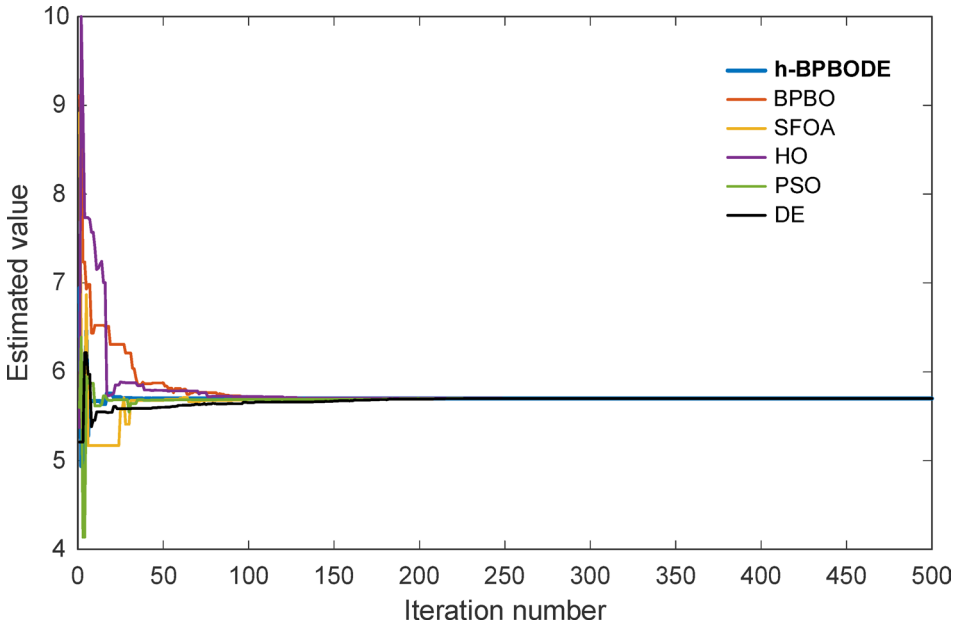


Fig. 17. Evolution of parameter c for Rössler system.

dispersion, and exact parameter recovery at the reporting precision. The consistency among the distributional statistics (Table 8), convergence curves (Fig. 14), parameter trajectories (Figs. 15, 16 and 17), and final estimates (Table 9) indicates that the proposed integration of DE operators within BPBO is effective in maintaining diversity while guiding the search efficiently to the correct parameter set.

Comparative analysis with recently reported variants of the PSO and DE algorithms

To further substantiate the competitiveness of the proposed h-BPBODE, an additional comparative analysis was conducted against four recently introduced and high-performing variants of PSO and DE algorithms: the dynamic explorative multi-operator differential evolution algorithm (DXMODE)[28], segmented mutation particle swarm optimization (SMPSO)[29], chaotic opposition-based-learning differential evolution with dynamic selection (CODEDS)[30], priority-driven search particle swarm optimization (PDPSO)[31]. These algorithms represent the latest generation of evolutionary optimizers that incorporate multiple mutation strategies, dynamic learning mechanisms, and adaptive population-management schemes to enhance exploration and convergence

Algorithm	a	b	c	MSE
h-BPBODE	0.200000	0.200000	5.700000	**0**
BPBO	0.200000	0.200000	5.700000	4.4285E−32
SFOA	0.200000	0.200000	5.700000	8.6520E−21
HO	0.199999	0.200055	5.700181	8.3002E−11
PSO	0.200000	0.200000	5.700000	3.0229E−18
DE	0.200000	0.200000	5.700000	1.6828E−16

Table 9. Parameters and MSE values obtained from different approaches for Rössler system. Significant values are in bold.

Algorithm	a	b	c	MSE
h-BPBODE	0.200000	0.200000	5.700000	**0**
FPA	0.199999972091997	0.200000170524519	5.69999976159705	4.1654E−07
IFFO	0.200000045139821	0.200000053226673	5.70000002921225	2.0942E−07
QPSO	0.199999999997114	0.200000000016239	5.69999999999965	2.1341E−11

Table 10. Comparative obtained parameters and MSE values with respect to reported approaches for Rössler system. Significant values are in bold.

System type	Algorithm	Minimum	Maximum	Median	Average	SD
Lorenz chaotic system	h-BPBODE	**0**	**1.8932E−28**	**0**	**2.1000E−29**	**4.6732E−29**
	DXMODE	1.1341E−29	3.8817E−18	4.8120E−20	4.9343E−19	1.0746E−18
	SMPSO	8.0466E−25	4.2826E−13	7.9365E−14	1.1037E−13	1.2565E−13
	CODEDS	2.3505E−27	1.7032E−11	2.5816E−14	2.0789E−12	4.5402E−12
	PDPSO	3.2948E−27	4.8810E−10	1.7867E−12	3.9267E−11	1.0597E−10
Chen chaotic system	h-BPBODE	**0**	**3.0957E−32**	**0**	**5.1046E−33**	**9.6463E−33**
	DXMODE	**0**	1.2130E−24	**0**	5.1145E−26	2.4229E−25
	SMPSO	2.1810E−22	7.4640E−13	1.3383E−20	2.9856E−14	1.4928E−13
	CODEDS	3.3193E−28	1.1073E−11	1.4365E−18	7.1817E−13	2.5500E−12
	PDPSO	4.3001E−26	5.5625E−12	9.5942E−16	3.9455E−13	1.2185E−12
Rössler chaotic system	h-BPBODE	**0**	**5.4232E−32**	**2.9986E−32**	**2.3735E−32**	**2.2511E−32**
	DXMODE	**0**	5.0657E−28	7.6111E−30	4.0998E−29	1.1452E−28
	SMPSO	2.6821E−31	1.4328E−18	7.3440E−26	5.8367E−20	2.8638E−19
	CODEDS	1.7568E−24	1.7641E−19	6.7936E−21	2.0489E−20	3.9382E−20
	PDPSO	1.3810E−24	4.0352E−13	4.7835E−17	4.6598E−14	1.1551E−13

Table 11. Comparative results of h-BPBODE and recent PSO/DE variants on chaotic systems. Significant values are in bold.

stability. Including them ensures that the proposed method is evaluated not only against classical baselines but also against the most recent developments in the field.

The comparative results summarized in Table 11 present the minimum, maximum, median, average, and standard-deviation (SD) values of the objective function obtained from 25 independent runs for each chaotic benchmark. Across all three systems (Lorenz, Chen, and Rössler) the proposed h-BPBODE achieves either exact-zero or near-zero objective values with minimal dispersion, clearly outperforming or matching the newly reported competitors. Specifically, for the Lorenz system, h-BPBODE attains an average objective of 2.10×10^{-29} with SD 4.67×10^{-29}, outperforming DXMODE (4.93×10^{-19}) and CODEDS (2.08×10^{-12}), and yielding markedly tighter convergence than PDPSO and SMPSO. For the Chen system, h-BPBODE again reaches a mean of 5.10×10^{-33} and SD 9.64×10^{-33}, surpassing all competitors whose averages remain above 10^{-26}. Likewise, for the Rössler system, the hybrid approach achieves a mean of 2.37×10^{-32} and SD 2.25×10^{-32}, demonstrating superior precision compared with DXMODE (4.10×10^{-29}), CODEDS (2.05×10^{-20}), and PDPSO (4.66×10^{-14}). These results confirm that the embedded DE refinement mechanism within BPBO enables the hybrid model to maintain robustness and convergence accuracy even when compared to advanced, dynamically adaptive PSO- and DE-based frameworks. From a broader perspective, this analysis validates that h-BPBODE not only retains a balanced exploration–exploitation trade-off but also sustains competitive performance across algorithmic generations. The findings underscore that its hybrid design (grounded in biologically inspired behavioral

modeling rather than purely mathematical mutation scheduling) provides a versatile and generalizable search capability applicable to complex nonlinear identification problems.

Conclusion

In this study, a hybrid birds of prey-based optimization with differential evolution was proposed to address the persistent challenges of parameter identification in chaotic systems. By embedding DE mutation and crossover operators within the four behavioral phases of BPBO, the hybrid framework successfully balanced exploration and exploitation, allowing every candidate update to be refined before acceptance. The method was validated on three canonical chaotic benchmarks (Lorenz, Chen, and Rössler) under a common experimental protocol and was compared against several established optimizers, including BPBO, SFOA, HO, PSO, and DE. The results demonstrated that h-BPBODE consistently achieved exact parameter recovery with negligible residuals, faster convergence, and markedly reduced variance across independent runs. Statistical analyses, convergence curves, and parameter evolution plots confirmed its superior robustness and precision, while cross-study comparisons further underscored its competitiveness against advanced hybrid, chaotic, and quantum-enhanced approaches.

Although the obtained results confirm that h-BPBODE is a reliable and efficient framework for chaotic parameter identification, several limitations of the present study should be acknowledged. The algorithm was validated primarily on three low-dimensional chaotic systems with idealized numerical conditions. Consequently, its scalability to high-dimensional or hyper-chaotic systems and its robustness under measurement noise or incomplete data remain to be examined. Moreover, the control parameter settings of the embedded DE operators were fixed throughout the simulations, which may restrict adaptability in highly irregular landscapes. In future work, these aspects may be addressed by (i) extending the method to complex and real-world chaotic models (e.g., electro-mechanical, biological, or financial systems); (ii) developing self-adaptive strategies for dynamically adjusting DE scaling and crossover rates within the BPBO cycle; (iii) investigating hybrid variants that combine h-BPBODE with chaos-driven or quantum-inspired mechanisms to further improve diversity maintenance; and (iv) integrating the algorithm into control and synchronization frameworks, enabling simultaneous identification and stabilization of nonlinear systems. These directions are expected to broaden the applicability of h-BPBODE beyond classical benchmarks and to establish a more general foundation for metaheuristic-based estimation and control of nonlinear dynamic processes.

Data availability

All corresponding data are presented within the manuscript.

Received: 17 September 2025; Accepted: 3 November 2025
Published online: 09 December 2025

References

1. Konnur, R. Synchronization-based approach for estimating all model parameters of chaotic systems. *Phys. Rev. E.* **67**, 027204. https://doi.org/10.1103/PhysRevE.67.027204 (2003).
2. Jafari, S., Sprott, J. C., Pham, V. T., Golpayegani, S. M. R. H. & Jafari, A. H. A new cost function for parameter estimation of chaotic systems using return maps as fingerprints. *Int. J. Bifurcat. Chaos.* **24**, 1450134. https://doi.org/10.1142/S021812741450134X (2014).
3. Clemente-López, D. et al. Poincaré maps for detecting chaos in fractional-order systems with hidden attractors for its Kaplan–Yorke dimension optimization. *AIMS Math.* **7**, 5871–5894. https://doi.org/10.3934/math.2022326 (2022).
4. Ko, C. N., Jau, Y. M. & Jeng, J. T. Parameter estimation of chaotic dynamical systems using HEQPSO. *J. Inf. Sci. Eng.* **31**, 675–689 (2015).
5. Chang, H., Feng, J. & Jiang, L. Novel hybrid optimization algorithm for parameter estimation of chaotic system. In *Proceedings of the 2016 International Forum on Mechanical, Control and Automation (IFMCA 2016)* (Atlantis Press, Paris, France, 2017). https://doi.org/10.2991/ifmca-16.2017.44
6. Ebrahimi, S. M., Malekzadeh, M., Alizadeh, M. & HosseinNia, S. H. Parameter identification of nonlinear system using an improved Lozi map based chaotic optimization algorithm (ILCOA). *Evol. Syst.* **12**, 255–272. https://doi.org/10.1007/s12530-019-09266-9 (2021).
7. Turgut, M. S., Sağban, H. M., Turgut, O. E. & Özmen, Ö. T. Whale optimization and sine–cosine optimization algorithms with cellular topology for parameter identification of chaotic systems and Schottky barrier diode models. *Soft Comput.* **25**, 1365–1409. https://doi.org/10.1007/s00500-020-05227-6 (2021).
8. Chen, Y., Pi, D. & Wang, B. Enhanced global flower pollination algorithm for parameter identification of chaotic and hyper-chaotic system. *Nonlinear Dyn.* **97**, 1343–1358. https://doi.org/10.1007/s11071-019-05052-z (2019).
9. Zainel, Q. M., Darwish, S. M. & Khorsheed, M. B. Employing quantum fruit fly optimization algorithm for solving three-dimensional chaotic equations. *Mathematics* **10**, 4147. https://doi.org/10.3390/math10214147 (2022).
10. Moreno-López, M. F. et al. FPGA implementation of PRNGs based on chaotic systems optimized by DE, GWO, and PSO. *Int. J. Circuit Theory Appl.* https://doi.org/10.1002/cta.4435 (2025).
11. Pérez-Cruz, J. H., Portilla-Flores, E. A., Niño-Suárez, P. A. & Rivera-Blas, R. Design of a nonlinear controller and its intelligent optimization for exponential synchronization of a new chaotic system. *Optik (Stuttg).* **130**, 201–212. https://doi.org/10.1016/j.ijleo.2016.10.140 (2017).
12. Dali, A., Abdelmalek, S., Bakdi, A. & Bettayeb, M. A class of PSO-tuned controllers in Lorenz chaotic system. *Math. Comput. Simul.* **204**, 430–449. https://doi.org/10.1016/j.matcom.2022.08.016 (2023).
13. Yau, H. T. & Chen, C. L. Chaos control of Lorenz systems using adaptive controller with input saturation. *Chaos Solitons Fract.* **34**, 1567–1574. https://doi.org/10.1016/j.chaos.2006.04.048 (2007).
14. Gotmare, A., Bhattacharjee, S. S., Patidar, R. & George, N. V. Swarm and evolutionary computing algorithms for system identification and filter design: A comprehensive review. *Swarm Evol. Comput.* **32**, 68–84. https://doi.org/10.1016/j.swevo.2016.06.007 (2017).
15. Gupta, S. et al. Estimation of parameters in fractional order financial chaotic system with nature inspired algorithms. *Procedia Comput. Sci.* **173**, 18–27. https://doi.org/10.1016/j.procs.2020.06.004 (2020).
16. Mehmood, K. et al. Design of chaos induced Aquila optimizer for parameter estimation of electro-hydraulic control system. *Comput. Model. Eng. Sci.* **143**, 1809–1841. https://doi.org/10.32604/cmes.2025.064900 (2025).
17. Mehmood, K. et al. Design of chaotic Young's double Slit experiment optimization heuristics for identification of nonlinear muscle model with key term separation. *Chaos Solitons Fract.* **189**, 115636. https://doi.org/10.1016/j.chaos.2024.115636 (2024).

18. Ghasemi, M. et al. Birds of prey-based optimization (BPBO): A metaheuristic algorithm for optimization. *Evol. Intell.* **18**, 88. https://doi.org/10.1007/s12065-025-01052-8 (2025).
19. Zhong, C. et al. Starfish optimization algorithm (SFOA): A bio-inspired metaheuristic algorithm for global optimization compared with 100 optimizers. *Neural Comput. Appl.* https://doi.org/10.1007/s00521-024-10694-1 (2024).
20. Amiri, M. H., Mehrabi Hashjin, N., Montazeri, M., Mirjalili, S. & Khodadadi, N. Hippopotamus optimization algorithm: A novel nature-inspired optimization algorithm. *Sci. Rep.* **14**, 5032. https://doi.org/10.1038/s41598-024-54910-3 (2024).
21. Marini, F. & Walczak, B. Particle swarm optimization (PSO). A tutorial. *Chemometr. Intell. Lab. Syst.* **149**, 153–165. https://doi.org/10.1016/j.chemolab.2015.08.020 (2015).
22. Das, S., Suganthan, P. N. & Evolution, D. A survey of the state-of-the-art. *IEEE Trans. Evol. Comput.* **15**, 4–31. https://doi.org/10.1109/TEVC.2010.2059031 (2011).
23. Maiti, B. et al. Enhanced crayfish optimization algorithm with differential evolution's mutation and crossover strategies for global optimization and engineering applications. *Artif. Intell. Rev.* **58**, 69. https://doi.org/10.1007/s10462-024-11069-7 (2025).
24. Cvitanović, P. Universality in Chaos, CRC Press, CRC Press Taylor & Francis Group 6000 Broken Sound Parkway NW, Suite 300 Boca Raton, FL 33487–2742 (2017). https://doi.org/10.1201/9780203734636
25. He, Q., Wang, L. & Liu, B. Parameter estimation for chaotic systems by particle swarm optimization. *Chaos Solitons Fract.* **34**, 654–661. https://doi.org/10.1016/j.chaos.2006.03.079 (2007).
26. Ho, M. C., Hung, Y. C. & Jiang, I. M. On the synchronization of uncertain chaotic systems. *Chaos Solitons Fract.* **33**, 540–546. https://doi.org/10.1016/j.chaos.2005.12.035 (2007).
27. Rössler, O. E. An equation for continuous chaos. *Phys. Lett. A.* **57**, 397–398. https://doi.org/10.1016/0375-9601(76)90101-8 (1976).
28. Reda, M., Onsy, A., Haikal, A. Y. & Ghanbari, A. A dynamic explorative multi-operator differential evolution algorithm for engineering optimization problems. *Inf. Sci. (N Y).* **717**, 122271. https://doi.org/10.1016/j.ins.2025.122271 (2025).
29. Zhang, X., Chen, Y., Cheng, L., Tian, S. & Liu, L. PSO with segmented mutation for site selection in grid-connected photovoltaic power generation system. *Appl. Energy.* **377**, 124352. https://doi.org/10.1016/j.apenergy.2024.124352 (2025).
30. Haro, E. H., Oliva, D., Beltrán, L. A. & Casas-Ordaz, A. Enhanced differential evolution through chaotic and Euclidean models for solving flexible process planning. *Knowl. Based Syst.* **314**, 113189. https://doi.org/10.1016/j.knosys.2025.113189 (2025).
31. Hu, G., He, P., Jia, H., Houssein, E. H. & Abualigah, L. Priority-driven search particle swarm optimization with dynamic candidate solutions management strategy for solving higher-dimensional complex engineering problems. *Comput. Methods Appl. Mech. Eng.* **446**, 118318. https://doi.org/10.1016/j.cma.2025.118318 (2025).

Author contributions

Serdar Ekinci, Davut Izci: Conceptualization, methodology, software, visualization, investigation, writing—original draft preparation. Murat Kayri, Fahmi Elsayed, Mohammad Salman: data curation, validation, supervision, writing—review and editing.

Funding

No funding was received for this work.

Declarations

Competing interests

The authors declare no competing interests.

Additional information

Correspondence and requests for materials should be addressed to D.I.

Reprints and permissions information is available at www.nature.com/reprints.

Publisher's note Springer Nature remains neutral with regard to jurisdictional claims in published maps and institutional affiliations.

Open Access This article is licensed under a Creative Commons Attribution-NonCommercial-NoDerivatives 4.0 International License, which permits any non-commercial use, sharing, distribution and reproduction in any medium or format, as long as you give appropriate credit to the original author(s) and the source, provide a link to the Creative Commons licence, and indicate if you modified the licensed material. You do not have permission under this licence to share adapted material derived from this article or parts of it. The images or other third party material in this article are included in the article's Creative Commons licence, unless indicated otherwise in a credit line to the material. If material is not included in the article's Creative Commons licence and your intended use is not permitted by statutory regulation or exceeds the permitted use, you will need to obtain permission directly from the copyright holder. To view a copy of this licence, visit http://creativecommons.org/licenses/by-nc-nd/4.0/.

© The Author(s) 2025